Applied Physics Letters

Effects of Ta incorporation in La_2O_3 gate dielectric of InGaZnO thin-film transistor

Cite as: Appl. Phys. Lett. **104**, 123505 (2014); https://doi.org/10.1063/1.4869761
Submitted: 25 December 2013 . Accepted: 17 March 2014 . Published Online: 26 March 2014

L. X. Qian, P. T. Lai, and W. M. Tang

ARTICLES YOU MAY BE INTERESTED IN

Effects of Ta incorporation in Y_2O_3 gate dielectric of InGaZnO thin-film transistor
Applied Physics Letters **109**, 163504 (2016); https://doi.org/10.1063/1.4965849

Low voltage operation of IGZO thin film transistors enabled by ultrathin Al_2O_3 gate dielectric
Applied Physics Letters **112**, 023501 (2018); https://doi.org/10.1063/1.5003662

High-mobility thin-film transistor with amorphous $\mathrm{InGaZn}O_4$ channel fabricated by room temperature rf-magnetron sputtering
Applied Physics Letters **89**, 112123 (2006); https://doi.org/10.1063/1.2353811

Lock-in Amplifiers
Find out more today

Zurich Instruments

© 2014 AIP Publishing LLC.

AIP Publishing

Effects of Ta incorporation in La_2O_3 gate dielectric of InGaZnO thin-film transistor

L. X. Qian,[1] P. T. Lai,[1,a)] and W. M. Tang[2]
[1]*Department of Electrical and Electronic Engineering, The University of Hong Kong, Pokfulam Road, Hong Kong*
[2]*Department of Applied Physics, The Hong Kong Polytechnic University, Hung Hom, Kowloon, Hong Kong*

(Received 25 December 2013; accepted 17 March 2014; published online 26 March 2014)

The effects of Ta incorporation in La_2O_3 gate dielectric of amorphous InGaZnO thin-film transistor are investigated. Since the Ta incorporation is found to effectively enhance the moisture resistance of the La_2O_3 film and thus suppress the formation of $La(OH)_3$, both the dielectric roughness and trap density at/near the InGaZnO/dielectric interface can be reduced, resulting in a significant improvement in the electrical characteristics of transistor. Among the samples with different Ta contents, the one with a Ta/(Ta + La) atomic ratio of 21.7% exhibits the best performance, including high saturation carrier mobility of 23.4 cm^2/V·s, small subthreshold swing of 0.177 V/dec, and negligible hysteresis. Nevertheless, excessive incorporation of Ta can degrade the device characteristics due to newly generated Ta-related traps. © *2014 AIP Publishing LLC*.
[http://dx.doi.org/10.1063/1.4869761]

Recently, amorphous InGaZnO (a-IGZO) thin-film transistors (TFTs) have been extensively explored for the application in various flat-panel displays.[1,2] Compared to conventional amorphous silicon or organic TFTs with a field-effect carrier mobility of ~1 cm^2/V·s,[3,4] a-IGZO TFTs typically exhibit a mobility higher than 10 cm^2/V·s,[5] which can translate to higher switching speed for electronic devices. In addition, a-IGZO TFTs offer better uniformity in device characteristics compared with polycrystalline silicon TFTs and have more excellent transparency to visible light than all the silicon-based devices.[6] In order to reduce their operating voltage, high-k materials have been adopted as gate dielectric in a-IGZO TFTs.[7,8] Among them, rare-earth oxide La_2O_3 is regarded as one of the most promising candidates due to its relatively high dielectric constant and large band gap (~6 eV).[9,10] However, La_2O_3 is hygroscopic, which can deteriorate both the dielectric constant and surface roughness of La_2O_3 film due to the formation of hydroxide $La(OH)_3$,[11] and thus induce degradations in the electrical characteristics of a-IGZO TFTs.[12] Fortunately, the doping of other elements, for example, Y, was reported to be an effective method to suppress the moisture absorption of La_2O_3 film.[13] In this work, the doping of Ta in La_2O_3 film is proposed due to the fact that Ta_2O_5 can exhibit both very high dielectric constant and excellent step coverage,[14] and accordingly the effects of Ta incorporation in La_2O_3 gate dielectric of a-IGZO TFTs are investigated. Three samples of a-IGZO TFTs with different Ta/(Ta + La) atomic ratios are prepared while one sample with pure La_2O_3 gate dielectric is also fabricated as the control sample.

Each sample was fabricated on a p-type (100) silicon wafer with a resistivity of 0.01–0.02 Ω·cm which acted as both the substrate and gate electrode. First, a 40-nm dielectric film was deposited by a sputtering system under a radio-frequency (RF) power supply for a ceramic target of La_2O_3 and a direct-current (DC) supply for a metal target of Ta in a mixed ambient of Ar plus O_2. The RF power was fixed at 40 W while the DC supply was set to be 0 A, 0.03 A, 0.04 A, and 0.05 A for sample_La_2O_3, sample_LaTaO_A, sample_LaTaO_B, and sample_LaTaO_C, respectively, so as to realize different atomic ratios of Ta/(Ta + La) in dielectric films. Second, an annealing treatment at 400 °C in an N_2 ambient for 30 min followed. Subsequently, the four samples received the deposition of a 60-nm a-IGZO active layer through RF sputtering from a ceramic target (Ga_2O_3: In_2O_3: ZnO = 1: 1: 1). After that, a lift-off process was utilized to form the source/drain electrodes, which were composed of 20-nm Ti and 80-nm Au. The channel width (W) and channel length (L) were 100 μm and 10 μm, respectively. Finally, all the samples were annealed in a forming-gas (N_2: H_2 = 95: 5) ambient at 350 °C for 20 min so that the contact resistance of the source/drain electrodes was reduced. In addition, metal-insulator-semiconductor capacitor was also prepared beside each sample to monitor the gate-oxide capacitance per unit area (C_{ox}). The current-voltage (I-V) curves of the TFTs were measured by a HP 4145B semiconductor parameter analyzer. Furthermore, the structural properties of the dielectric films were studied based on X-ray photoelectron spectroscopy (XPS) and atomic force microscopy (AFM).

Fig. 1 shows the XPS spectra of (a) La $3d_{5/2}$ and (b) O 1 s core levels for the dielectric films. The binding energies have been corrected for sample charging effect with reference to the C 1 s line at 285.0 eV. Accordingly to the XPS result, the atomic ratio of Ta/(Ta + La) is 0%, 21.7%, 30.6%, and 69.1% for sample_La_2O_3, sample_LaTaO_A, sample_LaTaO_B, and sample_LaTaO_C, respectively. As shown in Fig. 1(a), the La_2O_3 film exhibits an obvious shoulder at the high binding energy side of the La $3d_{5/2}$ main peak, suggesting the presence of La-OH bond due to the moisture absorption of La_2O_3. Furthermore, the La $3d_{5/2}$ peak of the La_2O_3 film (located at 834.7 eV) shifts to a higher binding energy compared to the ideal La_2O_3 reference peak (located at 834.0 eV) while being consistent with the reported peak for LaOOH film (located at 834.8 ± 0.2 eV) in peak location,[15] further revealing the

a)Electronic mail: laip@eee.hku.hk.

 © 2014 AIP Publishing LLC

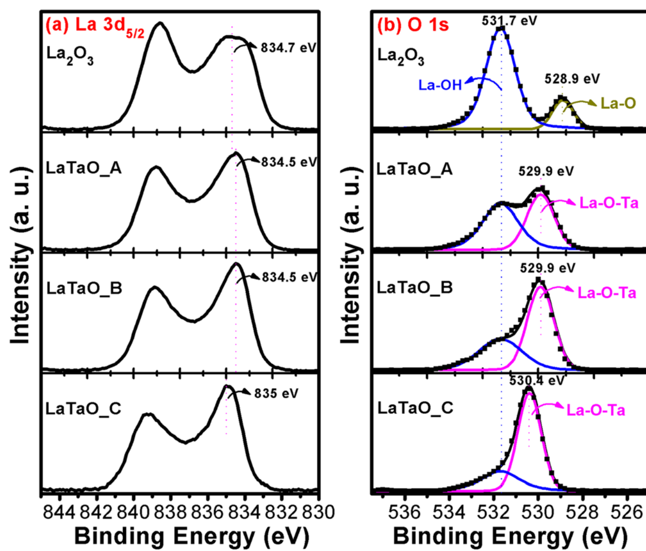

FIG. 1. XPS spectrum of (a) La $3d_{5/2}$ and (b) O 1 s for the dielectric films in sample_La_2O_3, sample_LaTaO_A, sample_LaTaO_B, and sample_LaTaO_C.

existence of $La(OH)_3$ in the La_2O_3 film. With Ta incorporation, the La $3d_{5/2}$ main peak becomes sharper, which is more obvious for higher Ta/(Ta + La) atomic ratio in the LaTaO film. This result is presumably due to the enhancement in the moisture resistance of the La_2O_3 film and accordingly the suppression in the formation of $La(OH)_3$ after Ta incorporation. Nevertheless, the La $3d_{5/2}$ peak related to sample_LaTaO_C (located at 835.0 eV) shifts to an even higher binding energy in comparison to sample_La_2O_3, suggesting the formation of La-O-Ta bond in the LaTaO film. The O 1 s spectra of the La_2O_3 and LaTaO films are shown in Fig. 1(b), and each fitting peak follows the general shape of the Lorentzian–Gaussian function. As for the La_2O_3 film, the two O 1s peaks correspond to La-O bond (located at 528.9 eV)[15] and La-OH bond (located at 531.7 eV), respectively. Moreover, the O 1 s peak corresponding to La-OH bond has a much higher intensity compared with that corresponding to La-O bond, indicating that most of La atoms in the La_2O_3 film have been transformed into $La(OH)_3$ due to moisture absorption. With Ta incorporation, the intensity of the O 1 s peak corresponding to La-OH bond decreases. Moreover, this effect becomes more obvious for higher Ta/(Ta + La) atomic ratio in the LaTaO film. This result further demonstrates the suppressed formation of $La(OH)_3$ due to the enhanced moisture resistance of the La_2O_3 film after Ta incorporation. Meanwhile, the O 1 s peak corresponding to La-O bond has been completely replaced by that corresponding to La-O-Ta bond (located at a higher binding energy) for each Ta-incorporated sample. Moreover, the O 1 s peak corresponding to La-O-Ta bond shifts to a higher binding energy with increased Ta/(Ta + La) atomic ratio as reflected by the comparison between sample_LaTaO_C and the other two Ta-incorporated samples, and similar effect also occurs to the La $3d_{5/2}$ spectrum in Fig. 1(a).

Fig. 2 shows the AFM images of the La_2O_3 and LaTaO films with a measurement area of 1 μm × 1 μm. The La_2O_3 film, with a RMS of 1.28 nm, exhibits the roughest surface among the dielectric films, which should result from non-uniform volume expansion of the La_2O_3 film after moisture absorption.[11] With Ta incorporation, the dielectric roughness is significantly reduced, which is more obvious for higher Ta/(Ta + La) atomic ratio. Accordingly, the RMS value of LaTaO film in sample_LaTaO_A, sample_LaTaO_B, and

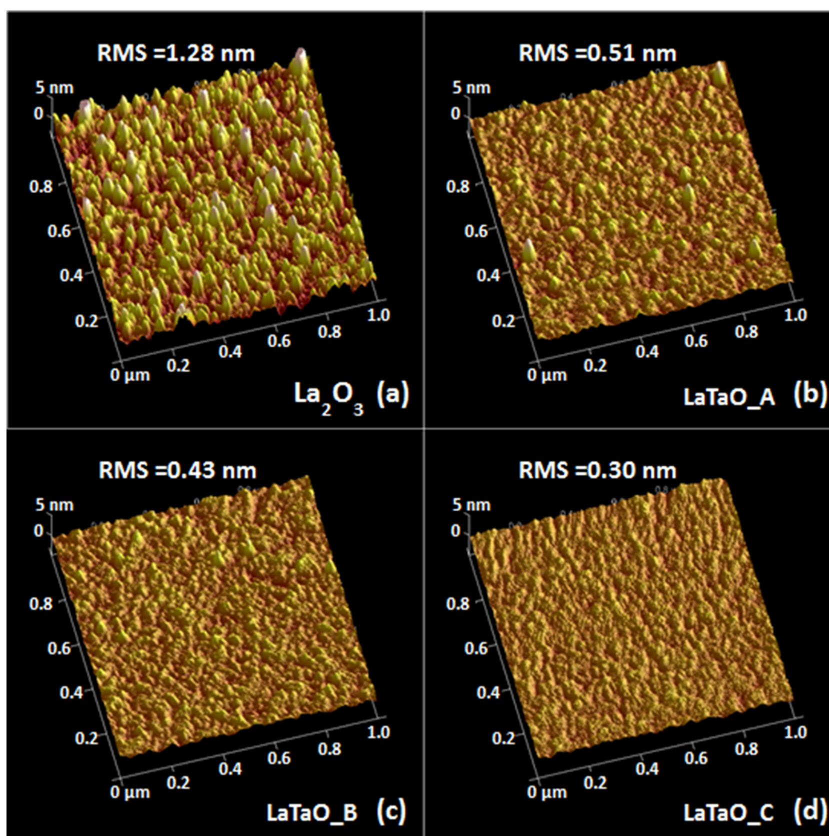

FIG. 2. AFM image of dielectric films in (a) sample_La_2O_3, (b) sample_LaTaO_A, (c) sample_LaTaO_B, and (d) sample_LaTaO_C.

TABLE I. Extracted electrical parameters of the a-IGZO TFT's.

Sample	La_2O_3	LaTaO_A	LaTaO_B	LaTaO_C
La deposition (RF/W)	40	40	40	40
Ta deposition (DC/A)	0	0.03	0.04	0.05
Atomic ratio of Ta/(Ta + La)	0%	21.7%	30.6%	69.1%
μ_{sat} (cm^2/V·s)	12.1	23.4	16.3	11.0
V_{TH} (V)	1.85	2.40	2.66	2.97
SS (V/dec)	0.234	0.177	0.201	0.217
ΔV_H (V)	−0.76	0.10	1.29	2.34
I_{on} (μA)	494	810	520	349
I_{on}/I_{off}	1.5×10^7	2.6×10^7	1.3×10^7	8.6×10^6
C_{ox} ($\mu F/cm^2$)	0.231	0.262	0.269	0.279
Dielectric constant	10.4	11.8	12.2	12.6

sample_LaTaO_C is 0.51 nm, 0.43 nm, and 0.30 nm, respectively, further demonstrating that Ta incorporation is an effective way to enhance the moisture resistance of La_2O_3 film and accordingly reduce its surface roughness. In addition, the enhanced moisture resistance of the La_2O_3 film also effectively suppresses the deterioration of its dielectric constant, and thus results in a continuous increase of dielectric constant associated with increasing Ta incorporation as listed in Table I. As compared to 3.9 of conventional SiO_2 dielectric, a larger dielectric constant of the LaTaO film (∼12) is conducive to achieving higher-performance TFT with smaller operating voltage and larger output current.

Fig. 3 exhibits the transfer characteristics of the a-IGZO TFTs: drain current (I_D) vs. gate-to-source voltage (V_{GS}) and $I_D^{1/2}$ vs. V_{GS} at a drain-to-source voltage (V_{DS}) of 5 V. The saturation carrier mobility (μ_{sat}), threshold voltage (V_{TH}), subthreshold swing (SS), on current (I_{on}), and on-off current ratio (I_{on}/I_{off}) of the devices are extracted from Fig. 3 and listed in Table I. Among them, μ_{sat} and V_{TH} are calculated from a linear fitting to the plot of $I_D^{1/2}$ versus V_{GS}, which is based on the I-V equation of field-effect transistor operating in the saturation region

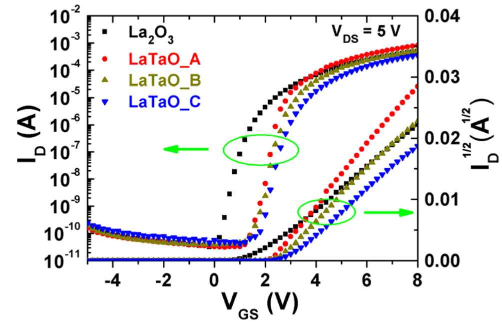

FIG. 3. Transfer characteristics of the a-IGZO TFTs in sample_La_2O_3, sample_LaTaO_A, sample_LaTaO_B, and sample_LaTaO_C.

$$I_D = (\mu_{sat} C_{ox} W/2L)(V_{GS} - V_{TH})^2. \quad (1)$$

By comparing sample_La_2O_3 and sample_LaTaO_A, μ_{sat} is nearly doubled from 12.1 cm^2/V·s to 23.4 cm^2/V·s with a reduction of SS from 0.234 V/dec to 0.177 V/dec due to the Ta incorporation in the La_2O_3 gate dielectric. It is believed that the reduction in dielectric roughness can induce a smoother a-IGZO/dielectric interface, thus resulting in an increase in carrier mobility due to reduced surface-roughness scattering on the carriers.[16] In addition, carrier mobility can also be improved by reducing the trap density at/near the a-IGZO/dielectric interface because of the restraint of electron trapping. Hence, the increase in μ_{sat} mentioned above can be attributed to smoother dielectric surface as well as lower trap density at/near the a-IGZO/dielectric interface, which are supported by the smaller values of RMS and SS, respectively.[1,17] Furthermore, it was reported that a large number of oxygen vacancies are easily generated in rare-earth oxide film due to the formation of hydroxide after reacting with moisture.[18] Hence, it is believed that the high trap density at/near the a-IGZO/dielectric interface in sample_La_2O_3 is related to the oxygen vacancies originated from the hygroscopicity of La_2O_3. In addition, a smaller V_{TH} (1.85 V) of sample_La_2O_3 in comparison to V_{TH} (2.40 V) of

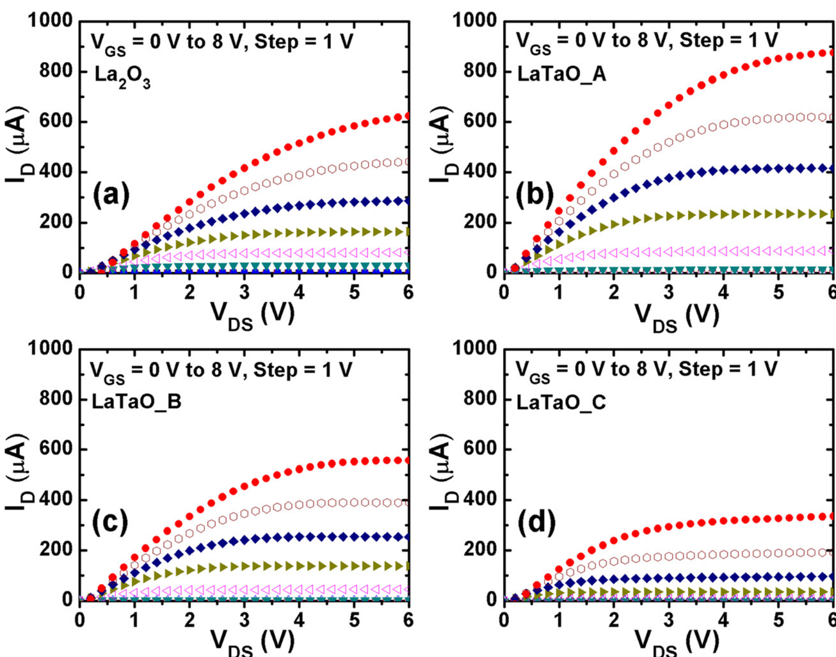

FIG. 4. Output characteristics of the a-IGZO TFTs: (a) sample_La_2O_3; (b) sample_LaTaO_A; (c) sample_LaTaO_B; and (d) sample_LaTaO_C.

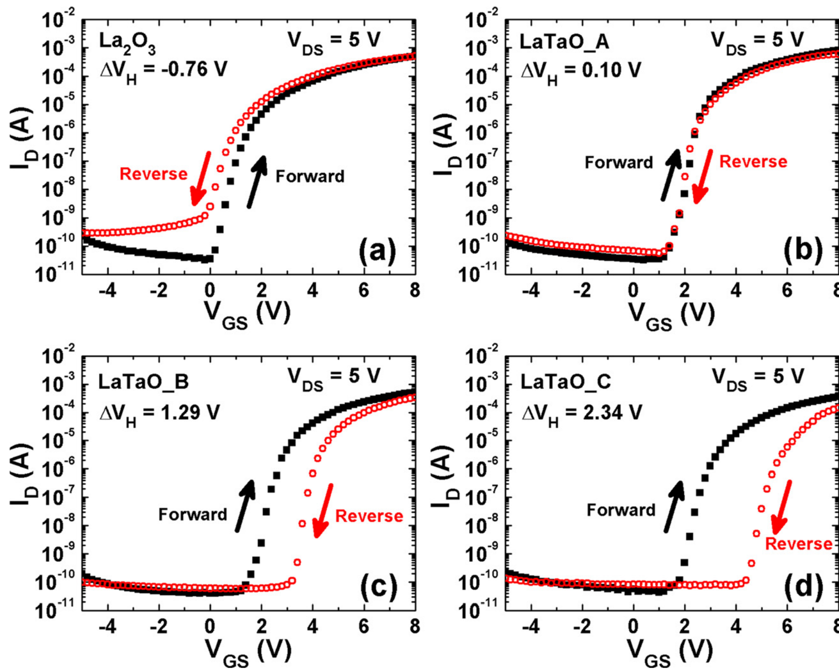

FIG. 5. Transfer characteristics of the a-IGZO TFTs measured under the forward and reverse V_{GS} sweepings: (a) sample_La_2O_3; (b) sample_LaTaO_A; (c) sample_LaTaO_B; and (d) sample_LaTaO_C.

sample_LaTaO_A can further reveal the existence of oxygen vacancies in the La_2O_3 gate dielectric as well as their reduction after Ta incorporation because oxygen vacancies can act as donor-like traps, inducing a negative shift of transfer curve and a degradation of SS in a-IGZO TFTs.[19] Besides, I_{on} and I_{on}/I_{off} are increased from 494 μA and 1.5×10^7 to 810 μA and 2.6×10^7, respectively, by Ta incorporation due to the improvement in carrier mobility. However, for further increase of Ta incorporation in the gate dielectric, the electrical characteristics of the TFT start to degrade even with a smoother dielectric surface, as reflected by the results of sample_LaTaO_B and sample_LaTaO_C. This should be ascribed to the creation of new Ta-related traps because a high density of defect states generally exists in Ta_2O_5 film,[20] which can be supported by the continual degradation of SS with increasing Ta/(Ta + La) atomic ratio in the LaTaO gate dielectric. Fig. 4 displays the output characteristics of the samples, which clearly exhibit an n-type enhancement mode. According to the comparison between sample_La_2O_3 and sample_LaTaO_A, the output current of the TFT is significantly increased by the Ta incorporation in the La_2O_3 gate dielectric due to the increase in carrier mobility. A continual reduction in output current with increasing Ta/(Ta + La) atomic ratio in the LaTaO gate dielectric is observed, which is consistent with the degradation in SS due to the generation of new Ta-related traps.

As shown in Fig. 5, the hysteresis properties of the samples are investigated according to the transfer characteristics measured under forward and reverse V_{GS} sweepings successively. ΔV_H is defined as the V_{TH} shift in the hysteresis loop. It is found that sample_La_2O_3 exhibits an obvious anticlockwise hysteresis with a negative ΔV_H (−0.76 V), further revealing the existence of donor-like traps at/near the a-IGZO/dielectric interface,[21] which is due to the introduction of oxygen vacancies in the La_2O_3 film after moisture absorption. These donor-like traps can induce electron-detrapping or hole-trapping and become positively charged[19] during the forward V_{GS} sweep of the hysteresis measurement. As a result, a decrease of V_{TH} is observed during the subsequent backward V_{GS} sweep. With Ta incorporation in the La_2O_3 gate dielectric, negligible hysteresis is exhibited by sample_LaTaO_A (ΔV_H = 0.10 V), which further demonstrates the reduction in the trap density at/near the a-IGZO/dielectric interface due to the enhanced moisture resistance of the dielectric film and thus suppressed generation of oxygen vacancies. In addition, the generation of new Ta-related traps, which are acceptor-like and prefer to capture electrons, has also been revealed by the continual enhancement of clockwise hysteresis with increasing Ta/(Ta + La) atomic ratio in the LaTaO gate dielectric. As a result, larger ΔV_H is exhibited by sample_LaTaO_B (ΔV_H = 1.29 V) and sample_LaTaO_C (ΔV_H = 2.34 V). A similar phenomenon of different signs of ΔV_H for hysteresis related to donor-like and acceptor-like traps has also been observed in other work.[22]

In this work, the impact of Ta incorporation in La_2O_3 gate dielectric on the electrical characteristics of a-IGZO TFT has been studied. It is found that Ta incorporation can effectively enhance the moisture resistance of the La_2O_3 film and suppress the formation of $La(OH)_3$, thus reducing the dielectric roughness as well as the trap density at/near the a-IGZO/dielectric interface. Accordingly, the electrical characteristics of the TFT are significantly improved as reflected by nearly doubled μ_{sat}, reduced SS, suppressed hysteresis, and increased output current. However, excessive incorporation of Ta in the gate dielectric can degrade the device characteristics due to the creation of new Ta-related traps. In summary, these results demonstrate the potential use of LaTaO gate dielectric for making high-performance a-IGZO TFTs.

This work was supported by the University Development Fund (Nanotechnology Research Institute, 00600009) of the University of Hong Kong.

[1] J. S. Park, W. J. Maeng, H. S. Kim, and J. S. Park, Thin Solid Films **520**, 1679 (2012).

[2]T. Kamiya, K. Nomura, and H. Hosono, Sci. Technol. Adv. Mater. **11**, 044305 (2010).
[3]R. A. Street, Adv. Mater. **21**, 2007 (2009).
[4]L. F. Deng, P. T. Lai, W. B. Chen, J. P. Xu, Y. R. Liu, H. W. Choi, and C. M. Che, IEEE Electron Dev. Lett. **32**, 93 (2011).
[5]H. Yabuta, M. Sano, K. Abe, T. Aiba, T. Den, H. Kumomi, K. Nomura, T. Kamiya, and H. Hosono, Appl. Phys. Lett. **89**, 112123 (2006).
[6]K. Nomura, H. Ohta, A. Takagi, T. Kamiya, M. Hirano, and H. Hosono, Nature **432**, 488 (2004).
[7]J. S. Lee, S. Chang, S. M. Koo, and S. Y. Lee, IEEE Electron Dev. Lett. **31**, 225 (2010).
[8]J. B. Kim, C. F. Hernandez, and B. Kippelen, Appl. Phys. Lett. **93**, 242111 (2008).
[9]J. Robertson, Eur. Phys. J. Appl. Phys. **28**, 265 (2004).
[10]C. H. Kao, H. Chen, J. S. Chiu, K. S. Chen, and Y. T. Pan, Appl. Phys. Lett. **96**, 112901 (2010).
[11]Y. Zhao, M. Toyama, K. Kita, K. Kyuno, and A. Toriumi, Appl. Phys. Lett. **88**, 072904 (2006).
[12]Y. J. Jo, I. H. Lee, and J. S. Kwak, Mater. Res. Bull. **47**, 2919 (2012).
[13]Y. Zhao, K. Kita, K. Kyuno, and A. Toriumi, Appl. Phys. Lett. **89**, 252905 (2006).
[14]S. C. Sun and T. F. Chen, IEEE Trans. Electron Dev. **44**, 1027 (1997).
[15]T. L. Barr, J. Phys. Chem. **82**, 1801 (1978).
[16]P. K. Nayak, M. N. Hedhili, D. Cha, and H. N. Alshareef, Appl. Phys. Lett. **100**, 202106 (2012).
[17]J. K. Jeong, J. H. Jeong, H. W. Yang, J. S. Park, Y. G. Mo, and H. D. Kim, Appl. Phys. Lett. **91**, 113505 (2007).
[18]F. H. Chen, J. L. Her, S. Mondal, M. N. Hung, and T. M. Pan, Appl. Phys. Lett. **102**, 193515 (2013).
[19]X. Xiao, W. Deng, S. Chi, Y. Shao, X. He, L. Wang, and S. Zhang, IEEE Trans. Electron Dev. **60**, 4159 (2013).
[20]S. Huang, IEEE Trans. Electron Dev. **60**, 2741 (2013).
[21]C. T. Tsai, T. C. Chang, S. C. Chen, I. Lo, S. W. Tsao, M. C. Hung, J. J. Chang, C. Y. Wu, and C. Y. Huang, Appl. Phys. Lett. **96**, 242105 (2010).
[22]L. X. Qian and P. T. Lai, IEEE Trans. Dev. Mater. Reliab. **14**, 177 (2014).